JOURNAL OF THERMOPHYSICS AND HEAT TRANSFER
Vol. 9, No. 4, October–December 1995

Effects of Upstream Wall Heating on Mixed Convection in Separated Flows

H. I. Abu-Mulaweh,* B. F. Armaly,† and T. S. Chen‡
University of Missouri–Rolla, Rolla, Missouri 65401

Measurements and predictions are reported for buoyancy-assisting, laminar mixed convection boundary-layer flow of air along a two-dimensional, vertical backward-facing step, in which the upstream wall and the step are heated to a uniform temperature while the downstream wall is heated to the same or different uniform temperature. The experiments were performed on a backward-facing step geometry, with a step height of 0.8 cm, over a range of freestream velocities $0.26 \leq u_\infty \leq 0.41$ m/s and a range of temperature differences $0 \leq \Delta T \leq 34$°C between the heated walls and the freestream. Laser Doppler velocimeter and cold-wire anemometer were utilized to measure, respectively, the air velocity and the temperature simultaneously. Flow visualizations were also performed to determine the flow reattachment length behind the backward-facing step. Reported measurements are limited to the case where the upstream wall and the step are heated to the same uniform temperature as the downstream wall, but numerical results are presented for the cases where these two temperatures are different and also for the situation when the upstream wall and the step are maintained as adiabatic surfaces. These results reveal that heating of the upstream wall and the step significantly affects the reattachment length, the velocity and temperature distributions, and the rate of heat transfer downstream of the backward-facing step.

Nomenclature

Gr_s = Grashof number, $g\beta(T_w - T_\infty)s^3/\upsilon^2$
g = gravitational acceleration
H = height of computational domain
h = heat transfer coefficient, $-k(\partial T/\partial y)_{y=0}/(T_w - T_\infty)$
k = thermal conductivity
Nu_s = local Nusselt number, hs/k
Re_s = Reynolds number, $u_\infty s/\upsilon$
T = fluid temperature
T_w = downstream wall temperature
T_{w1} = upstream wall/step temperature
T_∞ = freestream temperature
s = step height
U = dimensionless streamwise velocity component, u/u_∞
u, u_∞ = streamwise and freestream velocity component
X, Y = dimensionless streamwise and transverse coordinates, x/s, y/s
X_e, X_i, X_r = x_e/s, x_i/s, x_r/s
x_e = downstream heated length
x_i = inlet length upstream of the step
x_r = reattachment length
x, y = streamwise and transverse coordinates
α = thermal diffusivity
β = volumetric thermal expansion coefficient
ΔT = temperature difference, $(T_w - T_\infty)$
θ = dimensionless temperature, $(T - T_\infty)/(T_w - T_\infty)$
ξ = buoyancy parameter, Gr_s/Re_s^2
υ = kinematic viscosity

Received Dec. 20, 1994; revision received May 12, 1995; accepted for publication May 15, 1995.

*Lecturer in Mechanical Engineering, Department of Mechanical and Aerospace Engineering and Engineering Mechanics.

†Professor of Mechanical Engineering, Department of Mechanical and Aerospace Engineering and Engineering Mechanics. Member AIAA.

‡Curators' Professor of Mechanical Engineering, Department of Mechanical and Aerospace Engineering and Engineering Mechanics. Associate Fellow AIAA.

Introduction

FLOW separation and reattachment due to a sudden expansion in the flow passages play an important role in the design of heat transfer devices, such as cooling systems for electronic equipment, high-performance heat exchangers, chemical processes and energy systems equipment, cooling passages of turbine blades, and combustion chambers. Owing to its simple geometry, the backward-facing step flow geometry has received a great deal of attention in the literature, particularly for the forced convection case; see, e.g., Sparrow and Chuck[1] and the references cited therein. The mixed convection case has been explored recently by Baek et al.,[2] Abu-Mulaweh et al.,[3] and Hong et al.[4] These and other mixed convection studies considered the thermal boundary conditions of the upstream wall and the step as adiabatic, and the downstream wall as either at uniform temperature or at uniform heat flux. The influence of heating the upstream wall and the step on the mixed convection flow adjacent to a backward-facing step has not been explored experimentally or numerically, and this has motivated the present investigation.

The experimental component of this study focuses on a two-dimensional vertical backward-facing step geometry, shown schematically in Fig. 1, where the upstream wall and the step are heated to a uniform temperature that is equal to the temperature of the downstream heated wall (i.e., $T_{w1} = T_w$). We shall refer to this thermal boundary condition case as TBC-1. Measurements and predictions for the case where the upstream wall and the step were maintained adiabatic and the downstream wall was heated to a uniform temperature were reported earlier by Baek et al.,[2] and we shall refer to this thermal boundary condition as TBC-A. It was shown in that study that numerical predictions compared very favorably with measured results, thus justifying the use of the numerical model for predicting laminar flow and heat transfer characteristics in this geometry for conditions where measurements are not available. Based on that good comparison between measured and predicted results, the numerical model is used

Table 1 Summary of the various cases studied

Case	Description	Measurements	Computations
TBC-1	$T_{w1} - T_\infty = T_w - T_\infty$	Yes	Yes
TBC-A	Adiabatic upstream wall/step	Baek et al.[2]	Yes
TBC-2	$T_{w1} - T_\infty = 2(T_w - T_\infty)$	No	Yes
TBC-1/2	$T_{w1} - T_\infty = (T_w - T_\infty)/2$	No	Yes

in this study to explore the effects of upstream and step heating on the flow and heat transfer characteristics in this geometry. For that exploration, the step geometry, the freestream velocity, the freestream temperature, and the uniform temperature of the heated downstream wall are fixed and are identical for all the cases, while the heating conditions of the upstream wall and the step are varied for the different cases. Four upstream heating conditions were explored. The first two cases correspond to the TBC-1 and TBC-A conditions that were described previously. The third case corresponds to the conditions where the upstream wall and the step are heated to a uniform temperature, such that the temperature difference between the upstream wall and the freestream is twice that of the temperature difference between the downstream wall and the freestream, and we shall refer to this thermal boundary condition as the TBC-2 case. The fourth case corresponds to the conditions where the upstream wall and the step are heated to a uniform temperature, such that the temperature difference between the upstream wall and the freestream is half that of the temperature difference between the downstream wall and the freestream, and we shall refer to this thermal boundary condition as the TBC-1/2 case. As noted earlier, experiments were confined to the TBC-1 case. For clarity, a summary of these four different cases are presented in Table 1. The results for the velocity and temperature distributions, local Nusselt numbers, and reattachment lengths are presented and compared for all the previously mentioned thermal boundary conditions in order to assess the influence of upstream thermal boundary conditions on the flow and heat transfer characteristics in this geometry.

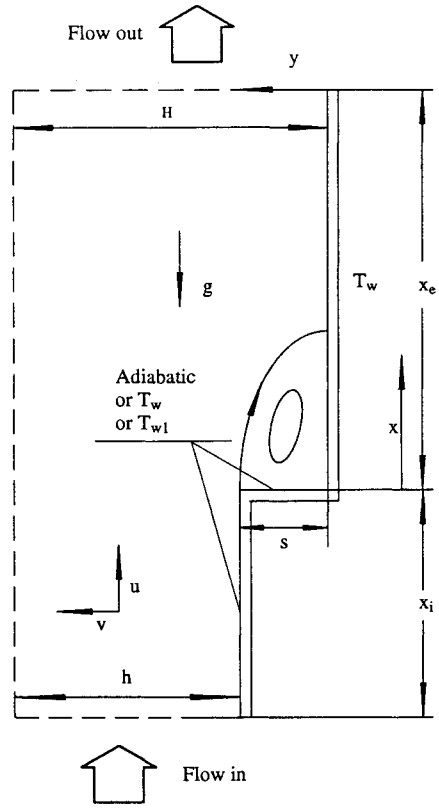

Fig. 1 Schematic diagram of the computational domain.

Experimental Apparatus and Analysis

The experimental study was carried out in an existing low-turbulence, open-circuit air tunnel. Details of the air tunnel have been described by Ramachandran et al.[5] In this experiment, the backward-facing step geometry in the test section of the tunnel was identical to that of Baek et al.[2] except that the upstream length and the step were also heated and maintained at the same uniform temperature as the downstream wall. The backward-facing step geometry was formed by an upstream section (30.48 cm long), a step (0.8 cm high), and a downstream section (79 cm long) behind the step. The test section (step geometry) spanned the entire width of the tunnel (30.48 cm) and the expansion ratio, the ratio of downstream height H to upstream height h above the test surface in the air tunnel, was equal to 1.056. The entire heated step geometry was instrumented with thermocouples and with heaters that were individually controlled to maintain the surface at any desired uniform temperature. The airflow velocities and temperatures were measured by a three-beam, backward-scattering, two-component laser Doppler velocimeter (LDV) and cold-wire anemometer, respectively. Only one velocity component (the streamwise velocity component) was measured in this study. Temperature and velocity measurements in the flow domain were made simultaneously by placing the cold wire probe about 2 mm behind the measuring control volume of the LDV system. The cold wire probe that was used in this study was a hot wire anemometer probe that operated in a constant current mode and was used as a resistance thermometer. The repeatability of the air velocity measurements was within 3% and that of the temperature measurements was within 0.05°C. Flow visualization was also conducted by utilizing a 15-W collimated white light beam, 2.5 cm in diameter, with glycerin particles seeding the flow. This flow visualization technique provided the capabilities of locally probing the flow domain for measuring the reattachment length.

The experimental geometry was also modeled for numerical simulation, as shown in Fig. 1, for the four different upstream thermal boundary conditions (TBC-1, TBC-A, TBC-1/2, and TBC-2) in a manner similar to that described by Abu-Mulaweh et al.,[3] where the solution procedure, convergence criterion, grid distributions, and numerical uncertainties are presented and discussed. In the present numerical simulation, x_i, x_e, s, and H were chosen to be 30.48, 40, 0.8, and 14 cm, respectively. The computation domain spanned from $-x_i < x < x_e$ and $0 < y < H$. The inlet boundary conditions at $x = -x_i$ were uniform velocity and temperature and the exit boundary conditions at $x = x_e$ were fully developed. Solutions were performed with nonuniform grid distributions and different grid densities to ensure grid-independent results. A grid density of $N_x \times N_y = 100 \times 80$ was found to be sufficient in providing a grid-independent result. For two mesh sizes of 100×80 and 140×120, the maximum changes in the predicted velocity, Nusselt number, and reattachment length were less than 3, 1.5, and 1%, respectively. The computations were performed on an Apollo 10000 computer and required 1000–1500 iterations in most cases to reach a converged solution to the coupled momentum and energy equations. Conver-

gence of the solution is considered satisfactory when the normalized sum of the residuals (mass, momentum, and energy) over the calculation domain is less than 0.005.

Results and Discussion

The experimental part of this study is limited to the thermal boundary conditions described as the TBC-1 case. The measured and predicted results of the TBC-1 case are compared with the predicted values from the numerical solution of Baek et al.[2] for the TBC-A case. In order to assess the effects of the upstream heating conditions, the measured and predicted results of the TBC-1 case are also compared with the predicted results of the TBC-1/2 and TBC-2 cases.

The boundary-layer flow development in the experimental apparatus, along with its two-dimensional nature, was verified through flow visualization and through measurements of velocity and temperature across the width of the air tunnel, at various heights above the test surface. These measurements showed a wide region (about 80% of the width of the heated test surface) around the center of the tunnel's width where the flow velocity is almost constant (to within 5%) at a fixed height above the heated test surface, thus justifying the two-dimensional flow approximation. All reported streamwise velocity and temperature distributions in the transverse y direction were taken along the midplane ($z = 0$) of the plate's width, and only after the system had reached steady-state conditions.

In this geometry, the velocity and temperature distributions at the step have been found to significantly affect the velocity and temperature distributions, reattachment lengths, and the heat transfer rate downstream of the step. Figure 2 presents

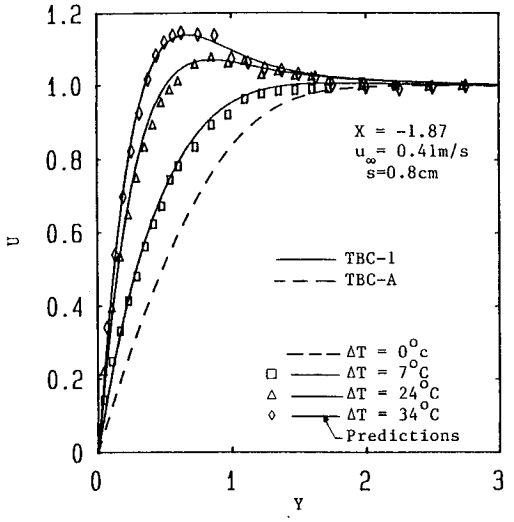

Fig. 2 Effects of upstream wall heating on the velocity distributions at $X = -1.875$ (uncertainty in U is ± 0.014 and in Y it is ± 0.022).

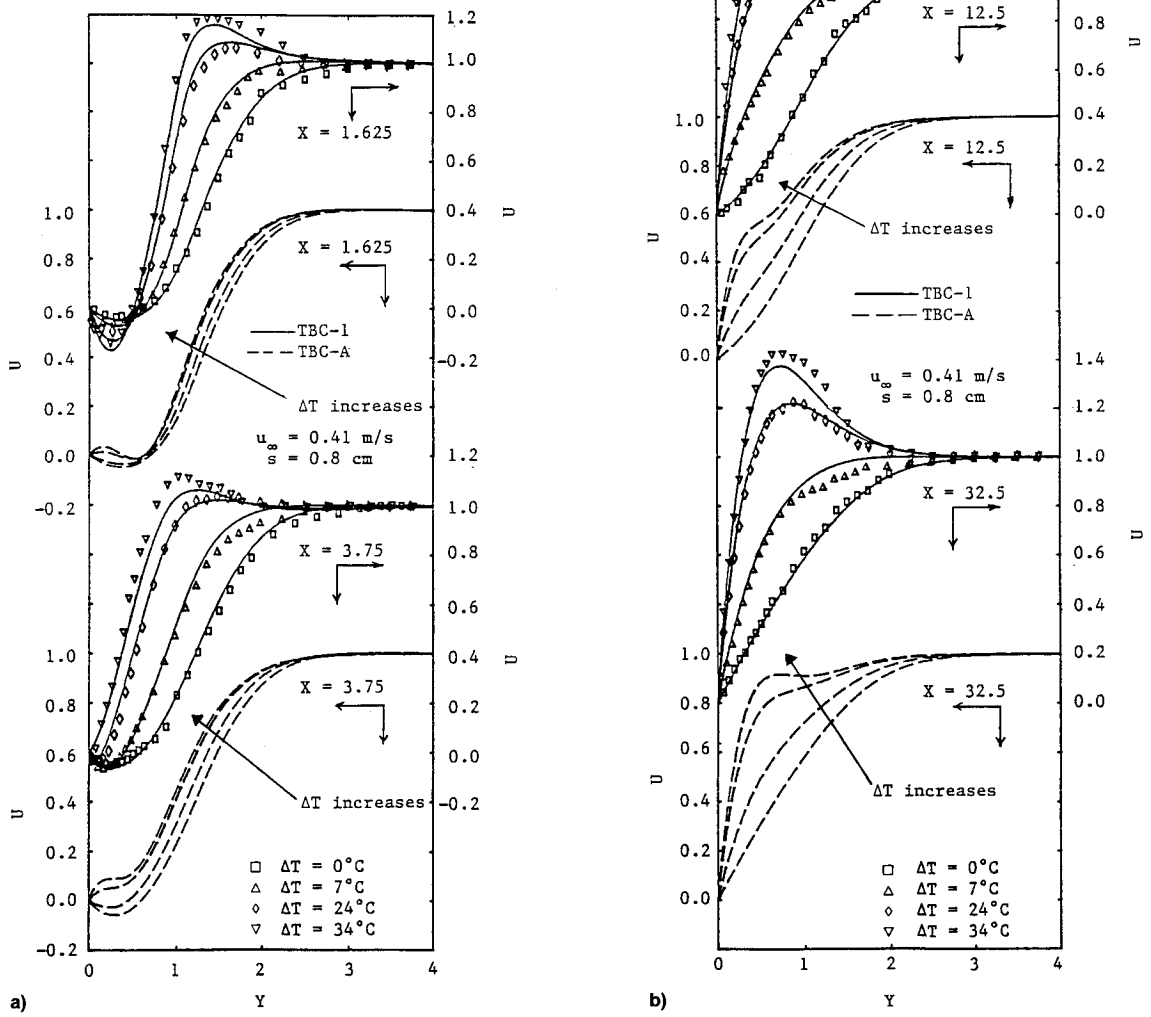

Fig. 3 Effects of upstream wall heating on the velocity distributions at X = a) 1.625 and 3.75 and b) 12.5 and 32.5 (uncertainty in U is ± 0.014 and in Y it is ± 0.022).

the measured and numerically predicted streamwise velocity distributions for the case of TBC-1 at a location upstream of the step, $X = -1.875$, for the freestream velocity $u_\infty = 0.41$ m/s and four different temperature differences ($\Delta T = 0$, 7, 24, and 34°C). The corresponding values of the local buoyancy force parameter Gr_x/Re_x^2 are 0, 0.39, 1.26, and 1.73, respectively. It should be noted that throughout this article the different symbols and different lines represent, respectively, the measured and predicted results. It is clear from this figure that the buoyancy force (i.e., heating the wall upstream of the step) significantly affects the streamwise velocity distribution upstream and at the edge of the step. The dashed line in this figure represents the predicted velocity distribution for the pure forced convection case ($\Delta T = 0$°C), which also represents the results of the TBC-A case. The solid lines represent the predicted velocity distributions for the TBC-1 case, which indicate a good agreement (within 5%) with measured values. As the temperature difference increases, the velocity gradient at the wall increases, and for high levels of buoyancy, i.e., for $\Delta T = 24$ and 34°C, the velocity inside the boundary layer becomes higher than the freestream velocity. This behavior of the velocity overshoot is similar to that reported by Ramachandran et al.[5] for mixed convection along a vertical flat plate.

Figures 3a and 3b present the measured and predicted velocity distributions at four different downstream locations from the step for the TBC-1 case, along with the predictions for the corresponding TBC-A case. The results show good agreements between the measured and predicted (solid lines) values. In the recirculation region, $X = 1.625$ (Fig. 3a), the magnitude of the velocity gradient at the wall (i.e., the shear stress) is seen to increase in the negative sense as the buoyancy force or ΔT increases for the TBC-1 case, while the opposite trend occurs for the TBC-A case. It should also be noted from Fig. 3a that for the TBC-A case at high temperature differences ($\Delta T = 24$ and 34°C), the streamwise velocity starts with a positive value adjacent to the heated wall, and then its magnitude becomes negative as the distance from the wall increases before it becomes positive again at farther distances from the heated wall. This behavior indicates that the recirculation region detaches from the heated wall at these high buoyancy levels for the TBC-A case, but that behavior was not observed for the TBC-1 case. It is also clear from the results that at $X = 3.75$ (Fig. 3a), the reattachment length decreases as the buoyancy level increases for both the TBC-1 and the TBC-A cases. It is evident from Fig. 3b that downstream of the reattachment point ($X = 12.5$ and 32.5) the velocity gradient at the heated wall (i.e., the shear stress) for the TBC-1 case is higher than the TBC-A case. In addition, the TBC-1 case exhibits velocity overshoots at higher temperature differences that are caused by the overshoot in the velocity distribution at the edge of the step as a result of heating the upstream wall. This overshoot in the velocity distribution was not observed for the TBC-A case.

The effects of freestream velocity on the velocity distributions downstream of the step are shown in Fig. 4. For the conditions presented in this figure, the velocity gradient at the wall increases with decreasing freestream velocity. This figure also shows that the dimensionless velocity in the region close to the wall is higher for lower freestream velocity, which is caused by the increased buoyancy force that results from decreasing the freestream velocity. For the TBC-A case the influence of the buoyancy force diminishes as the distance from the heated wall increases, causing that trend to reverse, while the influence of the buoyancy force for the TBC-1 case is felt throughout the velocity profile. It can also be seen that for the TBC-1 case, with the freestream velocity $u_\infty = 0.41$ m/s, the flow exhibits a negative velocity component at the streamwise location of $X = 3.75$, indicating that this location is upstream of the reattachment point and inside the recirculation region. On the other hand, for the TBC-A case at

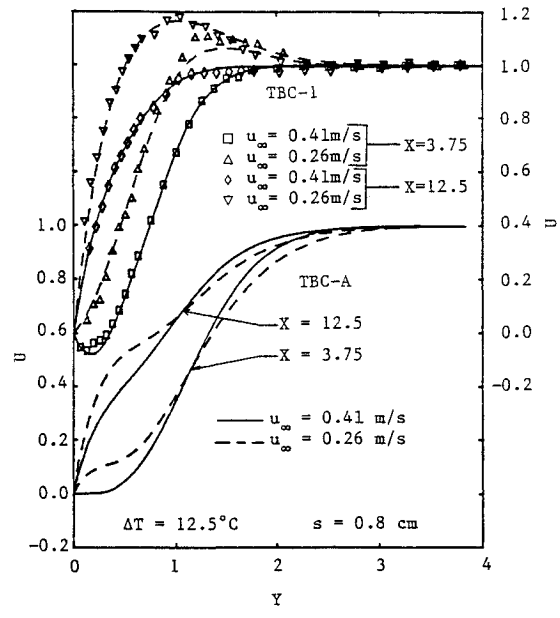

Fig. 4 Effects of upstream wall heating and freestream velocity on the velocity distribution (uncertainty in U is ±0.014 and in Y it is ±0.022).

the same location the velocity distribution does not exhibit any negative velocities, indicating that it is in the region downstream of the reattachment point. This means that for the conditions shown in the figure the reattachment length for the TBC-1 case is larger than that of the TBC-A case.

The temperature distributions at two locations downstream of the step are presented in Fig. 5 for the TBC-1 and TBC-A cases. It shows good agreement between the measured and predicted (solid lines) results for the TBC-1 case. As expected, owing to upstream heating, the thermal boundary-layer thickness downstream of the step for the TBC-1 case is larger than that of the TBC-A case. On the other hand, the temperature gradient at the wall (i.e., heat transfer rate) for the TBC-1 case is smaller than that of the TBC-A case due to the higher fluid temperatures that result from upstream heating. However, for both TBC-1 and TBC-A cases, the wall temperature gradient downstream of the step increases as the temperature difference increases.

The distribution of the local Nusselt number, as determined from the measured temperature gradient at the wall, is presented in Fig. 6 for different levels of buoyancy. The results indicate that for both TBC-1 and TBC-A cases, the Nusselt number increases (temperature gradients at the wall increase), with increasing temperature difference between the downstream wall and the freestream. However, for a given freestream velocity, step height, and temperature difference, the local Nusselt number for the TBC-1 case is considerably lower and the location of the maximum Nusselt number moves closer to the step than for the TBC-A case. Also, for the TBC-1 case, the Nusselt number distribution around the maximum surface seems to become steeper as the temperature difference increases. The results show that a fairly good agreement exists between the measured results and the numerical predictions (within 8%) for the TBC-1 case.

A more detailed examination of the effects of the thermal boundary conditions of the upstream wall and the step on the flow and heat transfer characteristics downstream of the step is performed through numerical simulations of the four different heating conditions that are specified by the TBC-A, TBC-1/2, TBC-1, and TBC-2 cases. In each case, the upstream wall and the step thermal boundary conditions were adjusted in the numerical solution to conform to their descriptions. In these numerically predicted results for the various cases, the freestream velocity was fixed at 0.41 m/s, the step height was

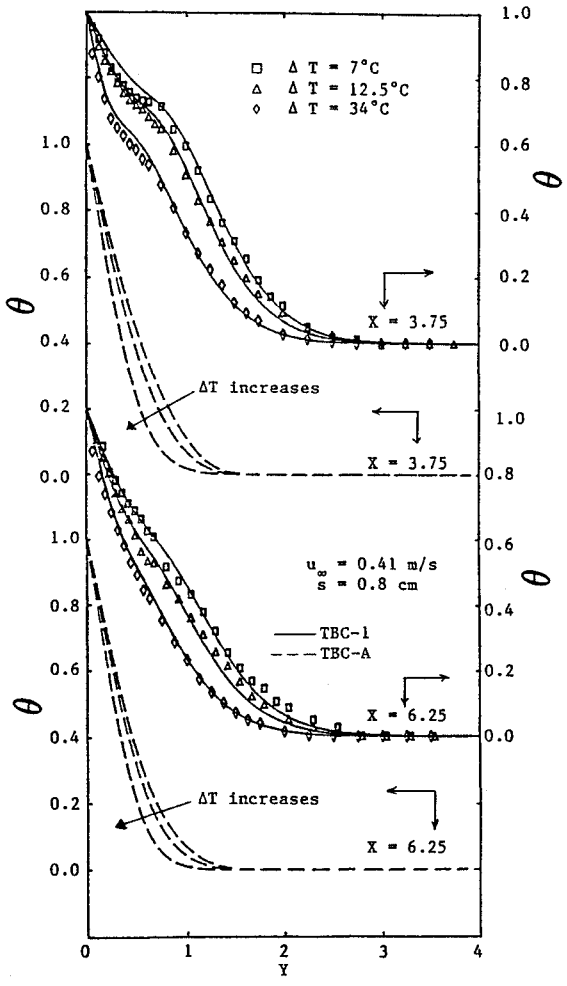

Fig. 5 Effects of upstream wall heating on the temperature distribution (uncertainty in Y is ±0.022 and in θ it is ±0.025).

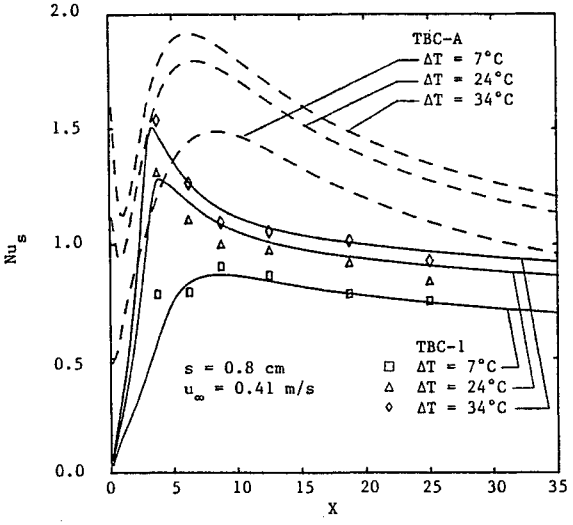

Fig. 6 Effects of upstream wall heating on the axial variation of the Nusselt number (uncertainty in Nu_s is ±0.05 and in X it is ±0.05).

fixed at 0.8 cm, and the temperature difference between the downstream wall and the freestream was fixed at 10°C. The thermal properties were considered to be constant in the numerical solution, but were evaluated at the film temperature of $T_f = (T_w + T_\infty)/2$, with freestream temperature fixed at 20°C. The velocity distributions for the four different cases at three different locations downstream from the step are presented in Fig. 7. It can be seen that upstream of the reattachment point ($X = 2.5$), the velocity gradient at the heated wall downstream of the step increases in the negative sense with increased heating of the upstream length and the step, whereas outside the recirculation region ($X = 6.25$ and 18.75) the velocity gradient increases in the positive sense with increased heating of the upstream length and the step. At high levels of heating of the upstream length and the step, corresponding to the TBC-2 case, the velocity distributions downstream of the step show an overshoot beyond the freestream value. This behavior is due to the velocity overshoot that exists at the step for this mixed convection flow condition, as is shown in Fig. 2.

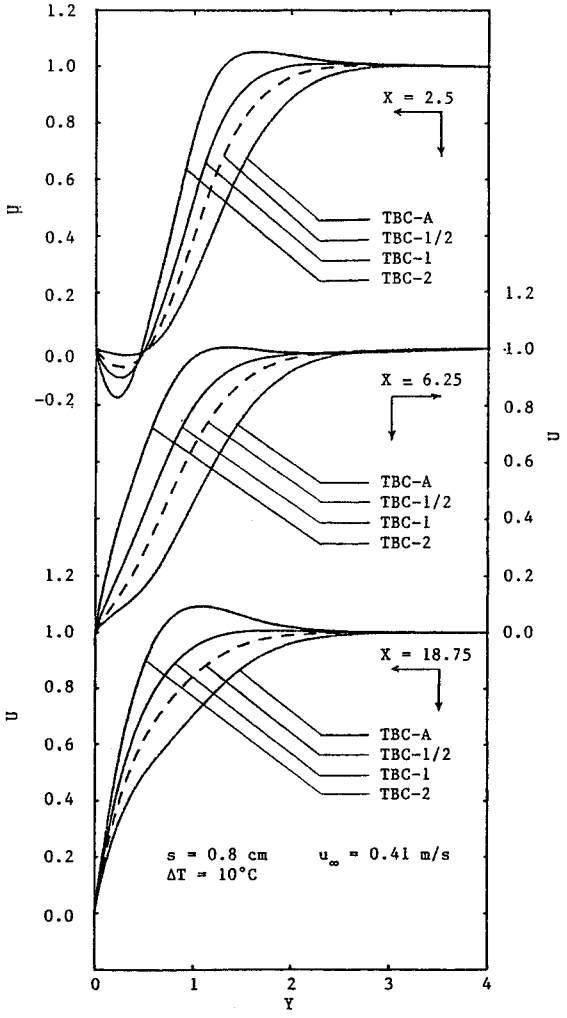

Fig. 7 Effects of upstream wall heating on the velocity distribution.

The temperature distributions for the same conditions as in Fig. 7 are presented in Fig. 8. The temperature gradient (i.e., the heat transfer rate) at the downstream wall decreases due to an increase in the fluid temperature as the heating level of the upstream wall and the step increases. As can be seen from the figure, for the case when the upstream wall and the step are heated to a higher temperature than the downstream wall (i.e., the TBC-2 case), the temperature gradient at the downstream wall close to the step (i.e., at $X =$ 2.5 and 6.25) is positive, while further downstream (i.e., at $X = 18.75$) it becomes negative. This behavior reflects the fact that at $X = 2.5$ and 6.25, heat is being transferred to the wall, rather than the reverse, as a result of higher fluid temperature that arises from a higher heating of the upstream wall and the step. Downstream from these locations, i.e., $X = 18.75$, the fluid that is heated by the upstream length and the step mixes with the lower temperature fluid of the freestream, causing that trend to reverse, and heat is then transferred from the wall to the fluid at this downstream location.

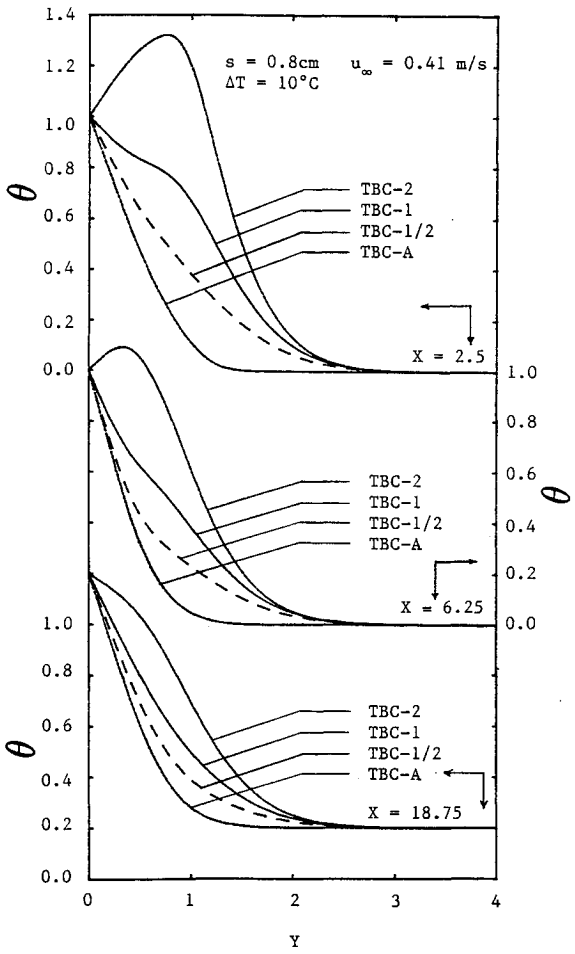

Fig. 8 Effects of upstream wall heating on the temperature distribution.

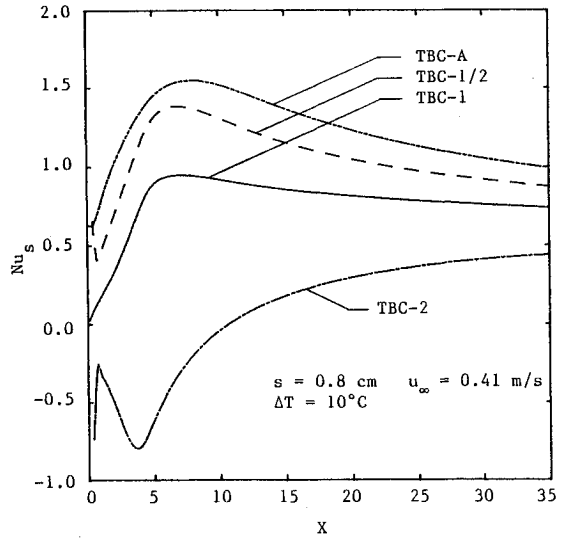

Fig. 9 Effects of upstream wall heating on the local Nusselt number.

The effects of thermal boundary conditions for the upstream length and step (i.e., TBC-A, TBC-1/2, TBC-1, and TBC-2) on the local Nusselt number distribution are presented in Fig. 9. The local Nusselt number downstream of the step decreases with increasing level of heating of the upstream wall and the step. This is due mainly to the increase in the fluid temperature caused by the heating of the upstream wall and step, which affects the temperature gradient at the wall. The TBC-2 case exhibits some interesting behavior near the step. The local Nusselt number in that region is negative, signifying that heat is being transferred from the fluid to the wall because of the positive temperature gradient at the wall. This is due to heating of the fluid by the higher temperature upstream wall and step, causing the fluid temperature in that region to become higher than that of the downstream wall. The heated step strongly influences the fluid temperature in its region, causing the heat transfer from the fluid to the wall to reach its maximum value at the lower corner of the step, i.e., $X = 0$. The rate of heat transfer from the fluid to the wall decreases first as the distance from the heated step increases. This trend is reversed, at some distance downstream from the step, when the fluid that is heated by the upstream wall starts mixing with the fluid that is heated by the step. Owing to the resulting higher fluid temperature in that region, the heat transfer from the fluid to wall starts to increase again with increasing distance from the step. This latter trend is then reversed as the distance from the step continues to increase, because the fluid that is heated by the upstream wall and the step is diluted by mixing with the lower temperature freestream fluid. The maximum negative value of the Nusselt number distribution for this case occurs at about one step height upstream of the reattachment region. This first causes the heat transfer from the fluid to the wall to decrease as the distance from the step increases until it becomes zero (i.e., $Nu_s = 0$) at approximately $X = 10$ (i.e., $x = 8$ cm). As the distance from the step continues to increase, the heat transfer direction is reversed so that heat is transferred from the heated downstream wall to the fluid. For the other three cases, TBC-1, TBC-1/2, and TBC-A, the maximum Nusselt number occurs at approximately two to four step heights downstream of the reattachment region.

Flow visualization was performed to determine the reattachment length for the TBC-1 case, and the numerical scheme was employed to predict the reattachment length for the TBC-A, TBC-1/2, and TBC-2 cases. The measured values for the TBC-1 case represent the average of several measurements that were taken under fixed conditions in order to reduce visualization errors. The uncertainty in these measurements is ±1 mm, which is less than 5% of the smallest measured reattachment length, and these results compared very well with predicted values. Figure 10 illustrates the predicted behavior of the reattachment length as a function of the buoyancy force parameter Gr_s/Re_s^2 for the cases of TBC-A, TBC-1, and TBC-2. The results of the TBC-1/2 case are not pre-

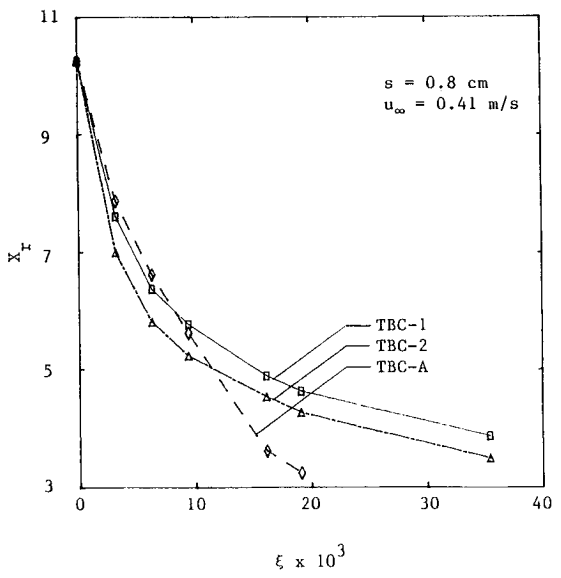

Fig. 10 Effects of upstream wall heating on the reattachment length (uncertainty in X_r is ±0.25 and in ξ it is $\pm 4 \times 10^{-5}$).

sented in this figure because they do not differ significantly from the results of the TBC-1 case. It can be seen that the reattachment length decreases as the buoyancy force parameter increases, and its magnitude for the TBC-1 case is higher than that of the TBC-2 case. At low levels of heating (i.e., small values of Gr_s/Re_s^2) the reattachment length of the TBC-A case is larger than either the TBC-1 case or the TBC-2 case, and its rate of decrease with buoyancy parameter is larger. The reattachment length results for the TBC-A case that are presented in this figure are confined to smaller values of Gr_s/Re_s^2 than the other cases. This is because for the TBC-A case the recirculation region detaches from the heated downstream wall at high levels of buoyancy parameter. On the other hand, for the TBC-1 and TBC-2 cases, the recirculation region remains attached to the heated downstream wall for the conditions examined in this study.

Conclusions

The effects of heating the upstream length and the step of a two-dimensional, vertical backward-facing step geometry on the flow and heat transfer characteristics in the region downstream of the step have been reported. It is clear from this study that the thermal boundary conditions of the upstream wall and the step affect significantly the temperature and velocity distributions, the local heat transfer rate, and the reattachment length for the mixed convection regime that was examined. For the buoyancy parameter range considered in this study, it has been found that the recirculation region remains attached to the heated wall downstream of the step when the upstream wall and the step are heated to the same or different uniform temperature as the downstream wall. It may, however, detach from the heated downstream wall at high buoyancy levels when the upstream wall and the step are treated as adiabatic surfaces. When the upstream wall and the step are heated to a higher temperature than the downstream wall, the velocity distribution downstream of the step may exhibit an overshoot over its freestream value. As expected, the heat transfer from the downstream wall to the fluid decreases as the upstream wall and the step are heated. The reattachment length decreases as the buoyancy level increases, with those for the higher upstream heating levels having the smaller reattachment lengths. The predicted results compare very well with the measured values.

Acknowledgments

The present study was supported in part by Grant NSF CTS-9304485 from the National Science Foundation. Bin Hong assisted in the numerical computations.

References

[1]Sparrow, E. M., and Chuck, W., "PC Solutions for Heat Transfer and Fluid Flow Downstream of an Abrupt, Asymmetric Enlargement in a Channel," *Numerical Heat Transfer*, Vol. 12, No. 1, 1987, pp. 19–40.

[2]Baek, B. J., Armaly, B. F., and Chen, T. S., "Measurements in Buoyancy-Assisting Separated Flow Behind a Vertical Backward-Facing Step," *Journal of Heat Transfer*, Vol. 115, No. 2, 1993, pp. 403–408.

[3]Abu-Mulaweh, H. I., Armaly, B. F., and Chen, T. S., "Measurements of Laminar Mixed Convection in Boundary-Layer Flow over Horizontal and Inclined Backward-Facing Steps," *International Journal of Heat and Mass Transfer*, Vol. 36, No. 7, 1993, pp. 1883–1895.

[4]Hong, B., Armaly, B. F., and Chen, T. S., "Mixed Convection in a Vertical Duct with a Backward-Facing Step: Uniform Wall Heat Flux Case," 1992 ASME Winter Annual Meeting, *Fundamentals of Mixed Convection*, HTD-Vol. 213, 1992, pp. 73–78.

[5]Ramachandran, N., Armaly, B. F., and Chen, T. S., "Measurements and Predictions of Laminar Mixed Convection Flows Adjacent to a Vertical Surface," *Journal of Heat Transfer*, Vol. 107, No. 3, 1985, pp. 636–641.